

Study of $K^- \rightarrow \pi^0 e^- \bar{\nu}_e \gamma$ decay with ISTRAP+ setup.

S.A. Akimenko^b, V. N. Bolotov^a, G. I. Brivich^b, K. V. Datsko^b, V. A. Duk^a,
A. P. Filin^b, E. N. Guschin^a, A. V. Inyakin^b, V. F. Konstantinov^b,
A. S. Konstantinov^b, I. Y. Korolkov^b, S. V. Laptev^a, V. A. Lebedev^a,
V. M. Leontiev^b, A. E. Mazurov^a, V. P. Novikov^b, V. F. Obraztsov^b,
V. A. Polyakov^b, A. Yu. Polyarush^a, V. E. Postoev^a, V. I. Romanovsky^b,
V. I. Shelikhov^b, O. G. Tchikilev^b, V. A. Uvarov^b, O. P. Yushchenko^b

^a Institute for Nuclear Research

INR RAS, prospekt 60-letiya Oktyabrya 7a, Moscow 117312, Russia

^b Institute for High Energy Physics

Protvino, Russia

10.10.2006

Abstract

Results of study of the $K^- \rightarrow \pi^0 e^- \bar{\nu}_e \gamma$ decay at ISTRAP+ setup are presented. 4476 events of this decay have been observed. The branching ratio (R) is found to be $R = \frac{Br(K^- \rightarrow \pi^0 e^- \bar{\nu}_e \gamma)}{Br(K^- \rightarrow \pi^0 e^- \bar{\nu}_e)} = (1.81 \pm 0.03(stat) \pm 0.07(syst)) \cdot 10^{-2}$ for $E_\gamma^* > 10 MeV$ and $\theta_{e\gamma}^* > 10^\circ$. For comparison with previous experiment the branching ratio with cuts $E_\gamma^* > 10 MeV$, $0.6 < \cos\theta_{e\gamma}^* < 0.9$ is measured $R = \frac{Br(K^- \rightarrow \pi^0 e^- \bar{\nu}_e \gamma)}{Br(K^- \rightarrow \pi^0 e^- \bar{\nu}_e)} = (0.47 \pm 0.02(stat) \pm 0.03(syst)) \cdot 10^{-2}$. For the cuts $E^*(\gamma) > 30 MeV$ and $\theta_{e\gamma}^* > 20^\circ$, used in most theoretical papers $Br = (3.06 \pm 0.09 \pm 0.14) \cdot 10^{-4}$. For the asymmetry A_ξ (for the same cuts as in Table.2) we get $A_\xi = -0.015 \pm 0.021$. At present time it is the best estimate of this asymmetry.

1 Introduction

The decay $K^- \rightarrow \pi^0 e^- \bar{\nu}_e \gamma$ provides fertile testing ground for the Chiral Perturbation Theory (ChPT) [1, 2]. $K^- \rightarrow \pi^0 e^- \bar{\nu}_e \gamma$ decay amplitudes are calculated at order ChPT $O(p^4)$ in [1], and branching ratios are evaluated in [3]. Recently next-to-leading $O(p^6)$ corrections were calculated for the corresponding neutral kaon decay [4].

The matrix element for $K^- \rightarrow \pi^0 e^- \bar{\nu}_e \gamma$ has general structure

$$T = \frac{G_F}{\sqrt{2}} e V_{us} \varepsilon^\mu(q) \left\{ (V_{\mu\nu} - A_{\mu\nu}) \bar{u}(p_\nu) \gamma^\nu (1 - \gamma_5) v(p_l) \right. \quad (1) \\ \left. + \frac{F_\nu}{2p_l q} \bar{u}(p_\nu) \gamma^\nu (1 - \gamma_5) (m_l - \not{p}_l - \not{q}) \gamma_\mu v(p_l) \right\} \equiv \varepsilon^\mu A_\mu.$$

First term of the matrix element describes Bremsstrahlung of kaon and direct emission (Fig.1a). The lepton Bremsstrahlung is presented by second term in r.h.s. of Eq(1) and (Fig.1b).

The $K^- \rightarrow \pi^0 e^- \bar{\nu}_e \gamma$ decay is one of kaon decays where new physics beyond the SM can be probed. This decay is especially interesting as it is sensitive to T-odd contributions.

According to CPT-theorem observation of T violation is equivalent to observation of CP-violating effects. CP violation is a subject of continuing interest in K and B meson decays.

In the SM the source of CP violation is given by the phase in the CKM matrix[5, 6, 7]. However it has been argued that this source is not enough to explain the observed baryon asymmetry of the universe and new sources of CP violation have to be introduced[8].

Important experimental observable used in CP-violation searches is the T-odd correlation for $K^- \rightarrow \pi^0 e \bar{\nu} \gamma$ decay defined as

$$\xi_{\pi e \gamma} = \frac{1}{M_K^3} p_\gamma \cdot [p_\pi \times p_e] \quad (2)$$

First suggestion to investigate T-odd triple-product correlations was done in[9]

To establish the presence of a nonzero triple-product correlations, one constructs a T-odd asymmetry of the form

$$A_\xi = \frac{N_+ - N_-}{N_+ + N_-} \quad (3)$$

Where N_+ and N_- are number of events with $\xi > 0$ and $\xi < 0$

T-odd correlation vanishes at tree level of SM[10], but the SUSY theory gives rise to CP-odd(T-odd) observables already at tree level[11, 12, 13]. T-odd asymmetry value for $SU(2)_L \times SU(2)_R \times U(1)$ model and scalar models was estimated in Ref[14].

In this letter we present first results of the analysis of the $K^- \rightarrow \pi^0 e \bar{\nu} \gamma$ data accumulated by ISTRA+ experiment during the 2001 run.

2 ISTRA+ setup

The experiment was performed using ISTRA+ detector which is modernized ISTRA-M detector [15]. ISTRA+ detector is located in a negative unseparated beam. The measurement of the beam particles, deflected by the beam magnet M1 is performed by four beam proportional chambers $BPC_1 \div BPC_4$. The beam momentum is $\sim 25 GeV$ with $\Delta p/p \sim 1.5\%$. Admixture of K^- in the beam is $\sim 3\%$. The beam intensity is $\sim 3 \cdot 10^6$ per 1.9 sec U-70 spill. The kaon identification is performed by $\check{C}_0 \div \check{C}_2$ threshold \check{C} -counters (\check{C}_0 is not shown in Fig.2).

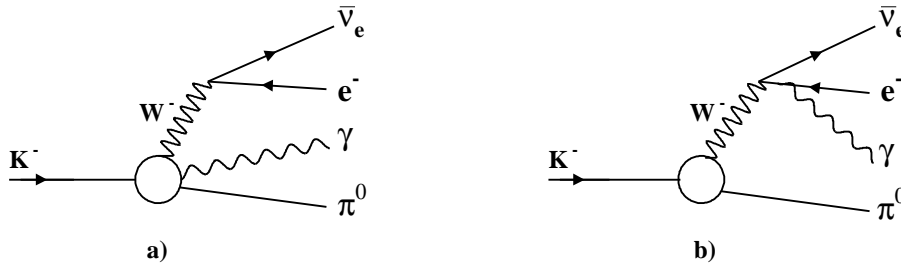


Figure 1: *Diagrammatic representation of the $K_{l3\gamma}$ amplitude.*

The decay products are deflected by the spectrometer magnet M2 with the field integral of 1Tm. The track measurement is performed by 1-mm-step proportional chambers ($PC_1 \div PC_3$), 2-cm-cell drift chambers ($DC_1 \div DC_3$), and by four planes of the 2-cm-diameter drift tubes DT. The photons are measured by lead-glass electromagnetic calorimeter SP_1 which consists of 576 counters. The counter transverse size is 5.2×5.2 cm and length is about $15 X_0$. To veto low energy photons the decay volume is surrounded by eight lead-glass rings. Lead-glass electromagnetic calorimeter SP_2 is also used as a part of the veto system.

3 Event selection

During physics run in November-December 2001 350M events were logged on tapes. This information is complemented by 260M events generated with Geant3 [16]. The Monte Carlo simulation includes a realistic description of the experimental setup: the decay volume entrance windows, the track chamber windows, gas mixtures, sense wires and cathode structures, Cherenkov counters mirrors and gas mixtures, the showers development in the electromagnetic calorimeters, etc. The detailed discussion of the simulation and reconstruction procedure is given in our previous publications [17, 18].

Events with one negative track detected in tracking system and four showers detected in electromagnetic calorimeter SP1 are selected as candidates for $K^- \rightarrow \pi^0 e \nu \gamma$ decay. One of this showers must be associated with the charged track.

Events with vertex inside interval $400 < z < 1650$ cm, and transverse radius less than 10cm is selected for further analysis.

The probability of the vertex fit, $CL(\chi^2)$, is required to be more than 10^{-4} . Absence of signals in veto system above noise threshold is required.

The electron identification is done using E/P ratio of the energy of the cluster associated with the track to momentum of this track given by tracking system. This ratio must be inside interval 0.80-1.15(see Fig.3). Another cut used for the suppression of the π^- contamination is that on the distance between the charged track extrapolation to the front plane of the electromagnetic detector and the nearest shower. This distance must be less than 2,5 cm.

The effective mass $m(\gamma\gamma)$ within ± 30 MeV from π^0 table mass (Fig.4) is required.

At the end, the convergence of the 2C $K^- \rightarrow \pi^0 e^- \bar{\nu}_e \gamma$ kinematic fit is required.

4 Background suppression

The main background decay channels for the decay $K^- \rightarrow \pi^0 e^- \bar{\nu}_e \gamma$ are:

- (1) $K^- \rightarrow \pi^- \pi^0 \pi^0$ where one of the π^0 photons is not detected and π^- decays to $e \nu$ or is misidentified as an electron.

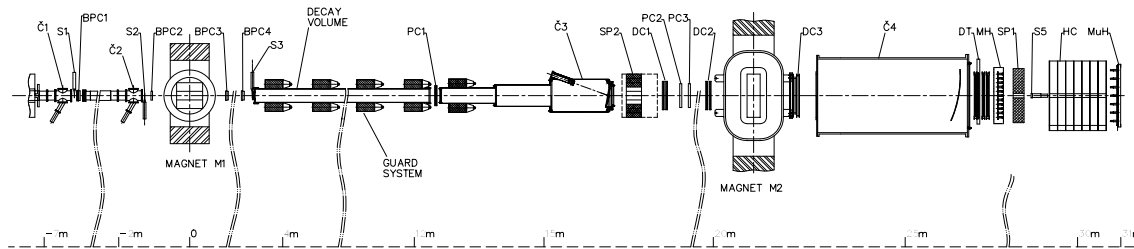


Figure 2: The side view of the ISTRA+ detector

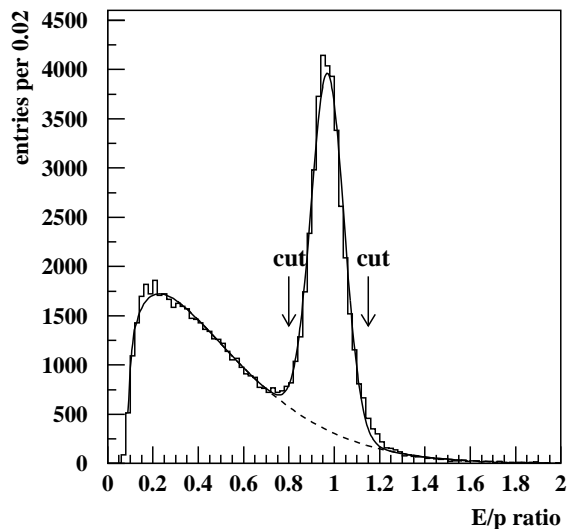


Figure 3: E/P ratio for the real data. Dotted line is our fit of background.

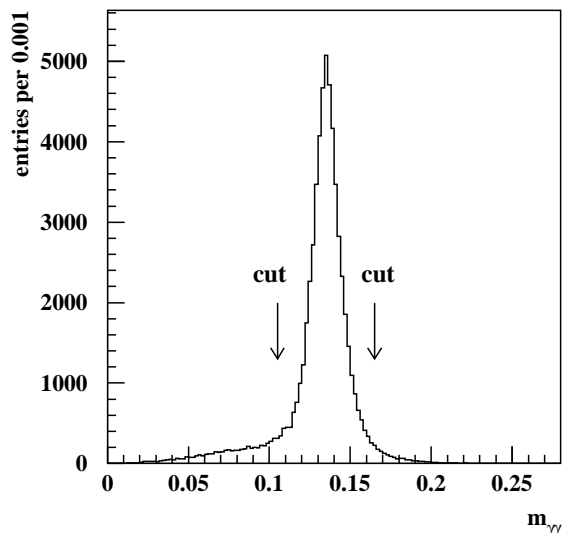


Figure 4: $\gamma\gamma$ mass for the real data.

(2) $K^- \rightarrow \pi^- \pi^0$ with “fake photon” and π^- decayed or misidentified as electron. Fake photon clusters can come from π -hadron interaction in the detector, external bremsstrahlung upstream of the magnet, accidentals. All these sources are included in our MC calculations.

(3) $K^- \rightarrow \pi^0 e \nu$ with extra photon. The main source of extra photons is an electron interactions in the detector.

(4) $K^- \rightarrow \pi^- \pi^0 \gamma$ when π^- decays or is mis-identified as an electron.

(5) $K^- \rightarrow \pi^0 \pi^0 e \nu$ when one γ is lost

From Fig.3 it is seen that in raw data background contamination from channels with charged pion in final state is about 15%.

Requirement on the missing energy in the decay reduces mainly background channel(4).

$$\text{Cut1: } E_{miss} > 0.5 \text{ GeV}$$

For the suppression of the background channels (1-5) we use a cut on the missing mass squared

$$M^2(\pi^0 e \gamma) = (P_K - P_{\pi^0} - P_e - P_\gamma)^2.$$

For the signal events this variable corresponds to the square of the neutrino mass and must be zero within measurement accuracy (see Fig.5).

$$\text{Cut2: } -0.01 < M^2(\pi^0 e^- \gamma) < 0.01$$

For the suppression of the background channel(1) we also use a cut on the missing mass squared $M^2(\pi^- \pi^0) = (P_K - P_{\pi^-} - P_{\pi^0})^2$

For the background(1) events this variable corresponds to π^0 mass, for the signal events distribution of this variable is rather wide (see Fig.6).

$$\text{Cut3: } \text{The events with } 0.009 < M^2(\pi^- \pi^0) < 0.024 \text{ are cutted out.}$$

The dominant background to $K_{e3\gamma}$ arises from K_{e3} with extra photon. The background (3) is suppressed by requirement on the angle between electron and photon in the laboratory frame $\theta_{e\gamma}$ (see Fig.7) The distribution of the K_{e3} -background events has

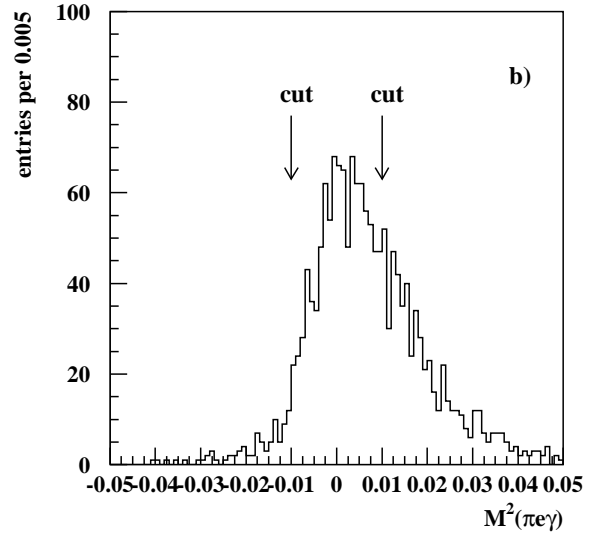
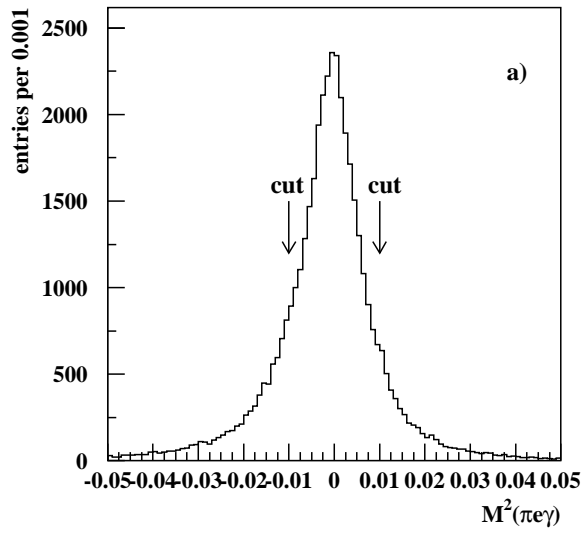


Figure 5: Missing mass $M^2(\pi^0 e^- \gamma)$ distribution; a) for the real data b) for the background channel(1).

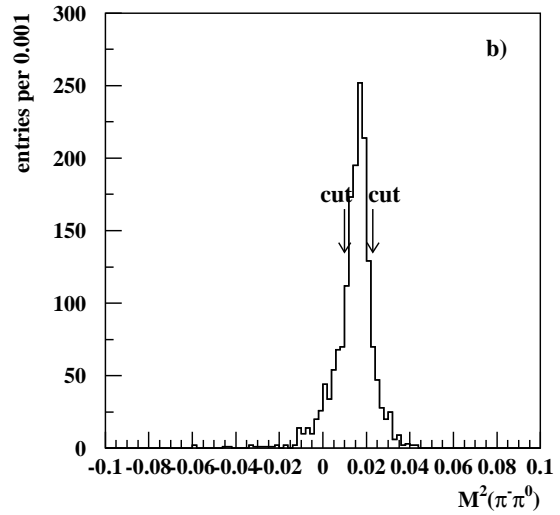
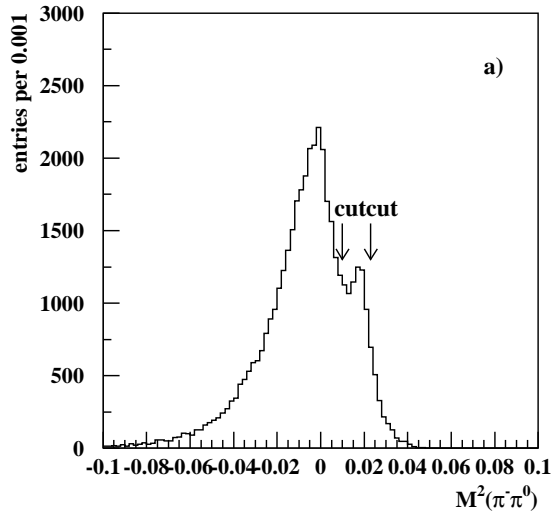


Figure 6: missing mass distribution $M^2(\pi^- \pi^0)$ a) for real data; b) for the background (1)

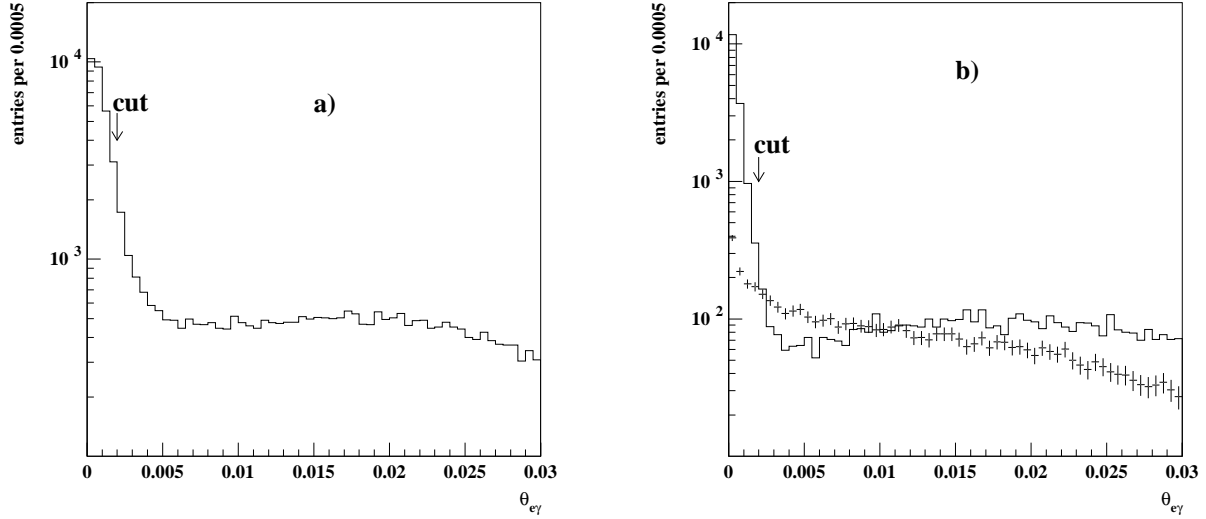


Figure 7: *Distribution over $\theta_{e\gamma}$ - the angle between electron and photon in lab. system. a) real data; b) MC background (histogram) and signal (points with errors)*

Cut	real data	background	signal MC
Number of events selected	41072	32901	11180
$E_{miss} > 0.5 GeV$	37428	31134	10035
$-0.01 < M^2(\pi^0 e^- \gamma) < 0.01$	26277	25287	8430
$0.09 < M^2(\pi^- \pi^0) < 0.24$	23293	21648	7153
$0.002 < \theta_{e\gamma} < 0.030$	6079	1603	4476

Table 1: *Event reduction statistics for the real data, the background MC and signal MC.*

very sharp peak at zero angle. This peak is significantly narrower than that for signal events. This happens, in particular, because the emission of the photons by the electron from K_{e3} decay occurs in the setup material downstream the decay vertex, but angle is still calculated as if emission comes from the vertex.

Cut4: $0.002 < \theta_{e\gamma} < 0.030$

Right part of this cut is introduced for suppression of background channels(1,2,4,5). After all cuts 6079 event are selected, with a background of 1603 events. Background normalization is done by comparison numbers of events for K_{e3} decay in MC and real data samples.

Event reductions statistics are summarized in Table 1.

5 Results

The resulting distribution of the selected events over $\cos\theta_{e\gamma}^*$, $\theta_{e\gamma}^*$ being the angle between the electron and the photon in the kaon rest frame is shown in Fig.8. The distribution over $E_{e\gamma}^*$ - the photon energy in the kaon rest frame is shown in Fig. 9. Reasonable agreement of the date with MC is seen. When generating the signal MC, a generator based on $O(p^2)$ [10] is used.

$R_{exp} \times 10^2$	ev numb	experiment
0.47 ± 0.02	1456	this exp.
0.46 ± 0.08	82	XEBC [19]
0.56 ± 0.04	192	ISTRA [20]
0.76 ± 0.28	13	HLBC [21]

Table 2: $Br(K^- \rightarrow \pi^0 e^- \bar{\nu}_e \gamma)/Br(K^- \rightarrow \pi^0 e^- \bar{\nu}_e)$ for $E(\gamma) > 10MeV, 0.6 < \cos\theta_{e\gamma} < 0.9$ in comparison with previous data.

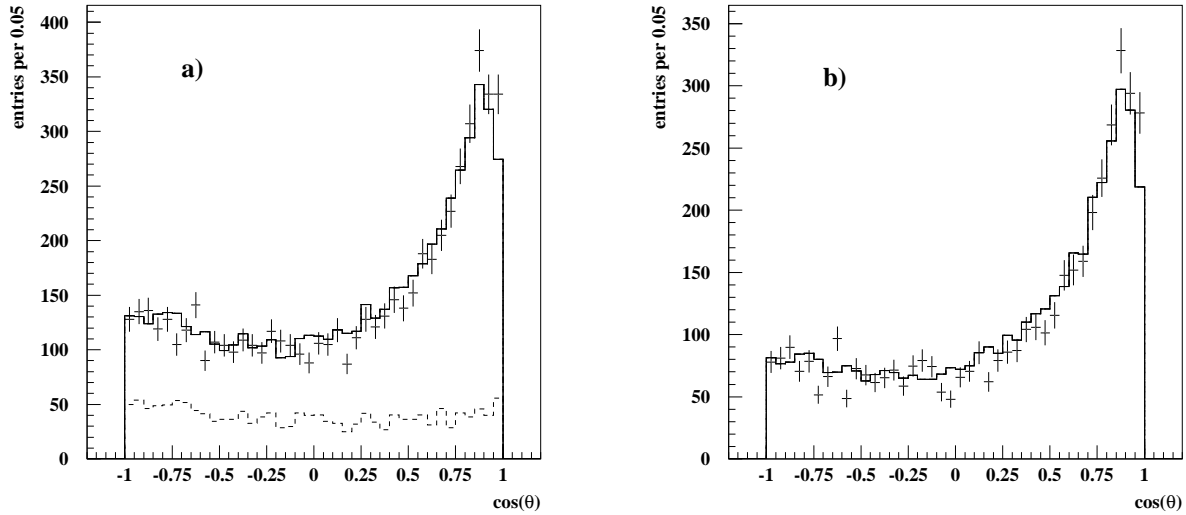


Figure 8: a) The distribution of the events over $\cos\theta_{e\gamma}^*$. Points with errors are the real data, histogram is - total MC signal plus background. Dotted line histogram is background. b) the same after background subtraction

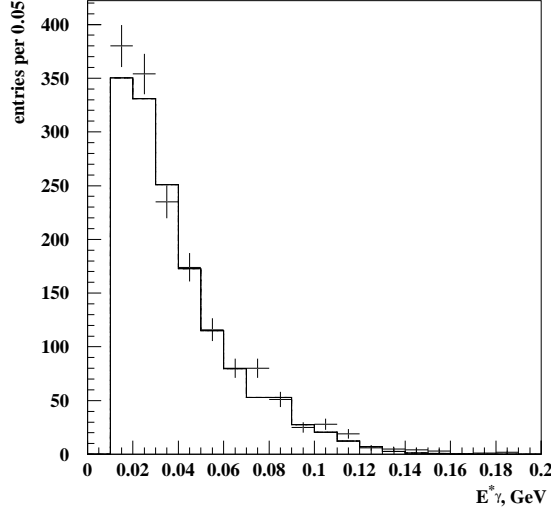


Figure 9: *The distribution of the events over E_γ^* - the energy of the photon in the kaon rest frame. Histogram corresponds to the data, points with errors- total signal plus background MC.*

To obtain the branching ratio of the $K_{\pi^0 e^- \bar{\nu}_e \gamma}$ relative to the K_{e3} (R), the background and efficiency corrected number of $K_{e3\gamma}$ events is compared to that of 569923 K_{e3} events found with the similar selection criteria. The branching ratio (R) is found to be

$$R = \frac{Br(K^- \rightarrow \pi^0 e^- \bar{\nu}_e \gamma)}{Br(K^- \rightarrow \pi^0 e^- \bar{\nu}_e)} = (1.81 \pm 0.03(stat) \pm 0.07(syst)) \cdot 10^{-2} \quad (4)$$

for $E_\gamma^* > 10 MeV$ and $\theta_{e\gamma}^* > 10^\circ$. Systematic errors are estimated by variation of the cuts of Table 1.

For comparison with previous experiment the branching ratio with cuts $E_\gamma^* > 10 MeV$, $0.6 < \cos\theta_{e\gamma}^* < 0.9$ is calculated

$$R = \frac{Br(K^- \rightarrow \pi^0 e^- \bar{\nu}_e \gamma)}{Br(K^- \rightarrow \pi^0 e^- \bar{\nu}_e)} = (0.47 \pm 0.02(stat) \pm 0.03(syst)) \cdot 10^{-2} \quad (5)$$

The results of previous experiments are given in Table.2

For the cuts $E^*(\gamma) > 30 MeV$ and $\theta_{e\gamma}^* > 20^\circ$, used in most theoretical papers

$$R = \frac{Br(K^- \rightarrow \pi^0 e^- \bar{\nu}_e \gamma)}{Br(K^- \rightarrow \pi^0 e^- \bar{\nu}_e)} = (0.64 \pm 0.02(stat) \pm 0.03(syst)) \cdot 10^{-2}. \quad (6)$$

Using PDG value for K_{e3} decay branching for $K^- \rightarrow \pi^0 e^- \bar{\nu}_e \gamma$ is calculated $Br = (3.06 \pm 0.09 \pm 0.14) \cdot 10^{-4}$. It can be compared with theoretical prediction[3] at tree level $Br = 2.8 \cdot 10^{-4}$ and $Br = 3.0 \cdot 10^{-4}$ for $O(p^4)$ level. Theoretical prediction of V.V.Braguta, A.A.Likhoded, A.E.Chalov[10] at tree level is $Br = 3.12 \cdot 10^{-4}$.

For the asymmetry A_ξ (for the same cuts as in Table.2) we get

$$A_\xi = -0.015 \pm 0.021 \quad (7)$$

At present it is the best estimate of this asymmetry. It can be compared with an upper limit on the A_ξ value $|A_\xi(K^- \rightarrow \pi^0 e^- \bar{\nu}_e \gamma)| < 0.8 \cdot 10^{-4}$ in the $SU(2)_L \times SU(2)_R \times U(1)$ model[14] and $A_\xi = -0.59 \cdot 10^{-4}$ in the Standard Model[10]

The authors would like to thank D.S. Gorbunov, V.A. Matveev and V.A. Rubakov, for numerous discussions. V.V.Braguta, A.A.Likhoded, A.E.Chalov for program of matrix element calculation. The work is supported in part by the RFBR grants N03-02-16330 (IHEP group) and N06-02-16065a (INR group).

References

- [1] J. Bijnens, G. Echer and J. Gasser, Nucl.Phys. B396 (1993) 81;
- [2] A. Pitch, Rep. Prog. Phys. 58 (1995) 563;
- [3] L.Maiani, G.Pancheri and N.Paver, The Second DAFNE Physics Handbook, (INFN-LNF-Divisione Ricerca, SIS-Ufficio Pubblicazioni, Frascati (Roma) Italy, ISBN 88-86409-02-8).
- [4] J. Gasser et.al ., arXiv:hep-ph/0412130
- [5] N. Cabibo Phys.Rev.Lett 10(1963)531
- [6] M. Kobayashi, T. Maskawa Progr.Theor. Phys. 49 (1973) 652.
- [7] C. Jarlskog Z.Phys. C29(1985)491.
- [8] G.F.Farrar and M.E.Shaposhnikov, Phys.Rev.Lett 70(1993)2833 [Erratum ibid 71(1993)210][arXiv:hep-ph/9305274]; P.Het and Sather, Phys.Rev D51(1995)379 [arXiv:hep-ph/9404302]; M.Carena, M.Quiros and C.E.Wagner, Phys.Lett. B380(1996) 81 [arXiv:hep-ph/9303420]
- [9] J.Gevas, J.Iliopolus, J.Kaplan Phys. Lett. 20(1966)432.
- [10] V.V.Braguta, A.A.Likhoded, A.E.Chalov, Phys. Rev. D 65(2002) 054038 [arXiv:hep-ph/0106147]
- [11] Y.Kuzuruki Phys. Lett., B193 (1987) 339.
- [12] A. Bartl, T.Kernreiter and W. Porod Phys Lett., B538 (2002) 59.
- [13] N. Oshimo Mod. Phys. Lett. A4 (1989) 145.
- [14] V.V.Braguta, A.A.Likhoded, A.E.Chalov Phys.Atom.Nucl.67:1003-1009,2004, Yad.Fiz.67:1025-1032,2004 [arXiv:hep-ph/0305067]
- [15] V.N.Bolotov et.al ., IHEP preprint 8-98, 1998.
- [16] R.Brun et al ., Preprint CERN-DD/EE/84-1.
- [17] I.V.Ajinenko et al ., Yad. Fiz 65(2002) 2125; I.V.Ajinenko et al ., Phys. At. Nucl., 66 (2003) 2064 I.V.Ajinenko et al ., Phys Lett., B574 (2003) 14. O.P.Yuschenko et al ., Phys Lett., B589 (2004) 111.
- [18] I.V.Ajinenko et al ., Yad. Fiz 66(2003) 107; I.V.Ajinenko et al ., Phys. At. Nucl., 66 (2003) 105 O.P.Yuschenko et al ., Phys Lett., B581 (2004) 159.
- [19] V.V.Barmin et.al ., SJNP 55(1991) 547, 53(1991)976.
- [20] V.N.Bolotov et.al ., JETPL 42(1985)481, Yad. Fiz 44(1986)108.
- [21] F.Romano et.al ., Phys Lett., 36B(1971)525.